Computer-Integrated Surgery (CIS) I
October 4, 2022
Hackerman B17

Bringing "the sixth sense" for surgeons using light and sound

Jeeun Kang, Ph.D.

JOHNS HOPKINS UNIVERSITY

LABORATORY FOR Computational Sensing + Robotics

MUSiiC Research Laboratory

1

Evolution of my personal interest

- **One-dimensional advances towards smaller clinical ultrasound (US) imaging**

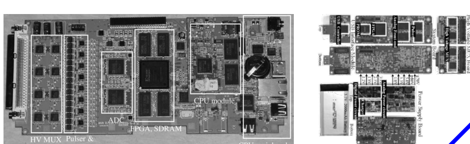

Could be more colorful?

Could be nimbler in catching subtle temporal changes?

- **Multi-modal imaging**

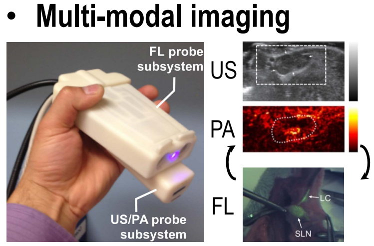

- **Higher spatiotemporal-spectral contrast**

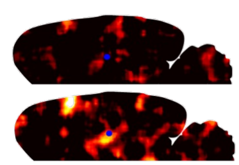

Neuroimaging

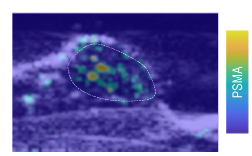

Tumor-targeted imaging

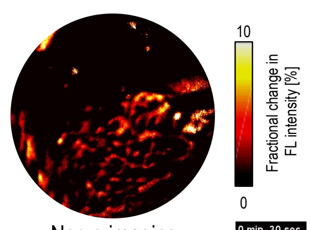

Nerve imaging

2

2

Defining the right form of "the sixth sense"

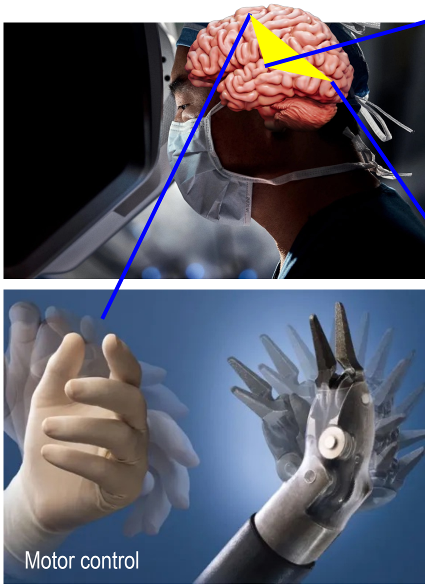

Knowledge in human anatomy &
body memory of surgical procedures

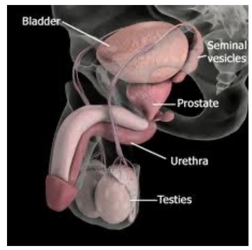

Vision: a dynamic input

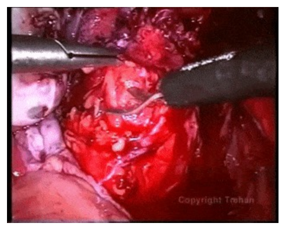

Crisp perception is a must for the new sixth sense

- High spatiotemporal resolution
- High contrast resolution
- Wide volumetric field-of-view
- Real-time feedback
- No surgical interruption

3

3

Current state-of-the-art in intra-operative guidance

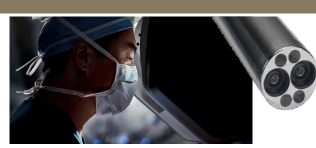

White light **Fluorescence**

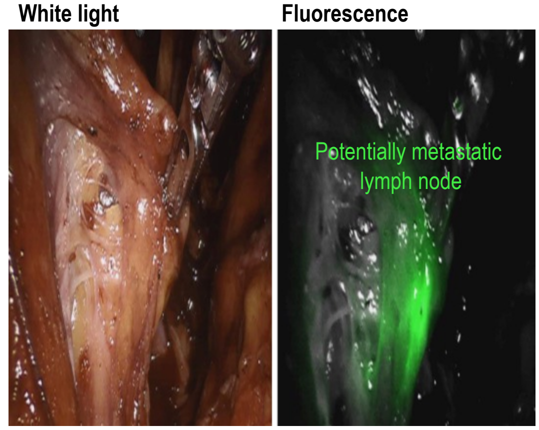

Transverse plane

4

† Manny, T. B., Patel, M. & Hemal, A. K. *Eur Urol* **65**, 1162–1168 (2014).

4

Current state-of-the-art in intra-operative guidance

Fluorescence imaging †

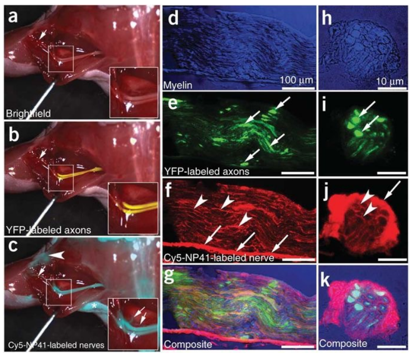

- Only 2-dimensional perception with *en face* imaging FOV

Confocal / multiphoton microscopy & Raman spectroscopy

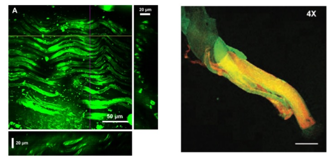

- Slow imaging
- Limited imaging depth & FOV

Optical coherence tomography (OCT) ‡

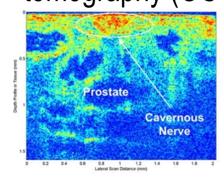

- Small FOV in few mm diameter
- Limited contrast resolution

X-ray §

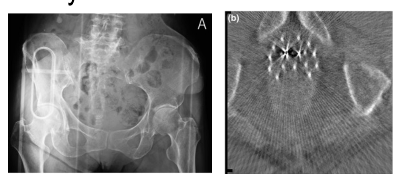

- Ionizing effect
- Interrupt the surgical procedure

Prostate MRI §

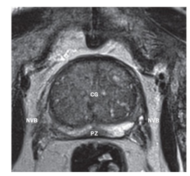

- Challenging for intra-operative use

† Whitney, M. A. et al. Nat Biotechnol 29, 352–356 (2011).
‡ Chitchian, S., et al., J. Biomed. Opt. 14, 014031-14-6 (2009).
§ A. L. Burnett, Nat. Rev. Urol. 12, 451-460 (2015).

5

5

Medical ultrasound

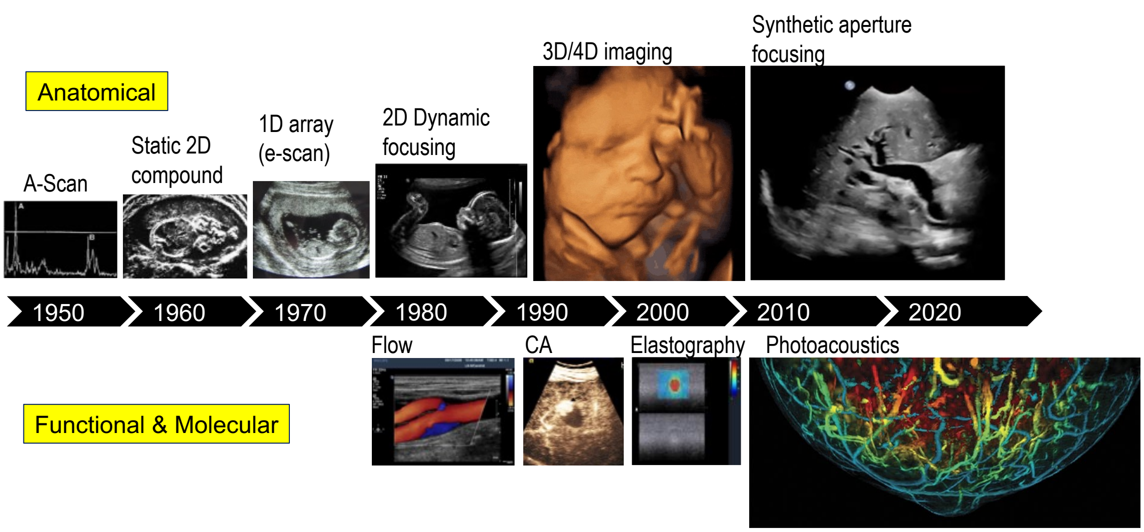

6

6

Prostate Cancer (PCa)

- PCa is a **leading organ for new cancer cases** for males, (21% in total cancer diagnosis) resulting **second highest cancer deaths** †
- High survival rate when localized, but **survival rate drops with metastasis**
- **Early PCa detection & accurate surgery for negative tumor margin** are the best defense strategy

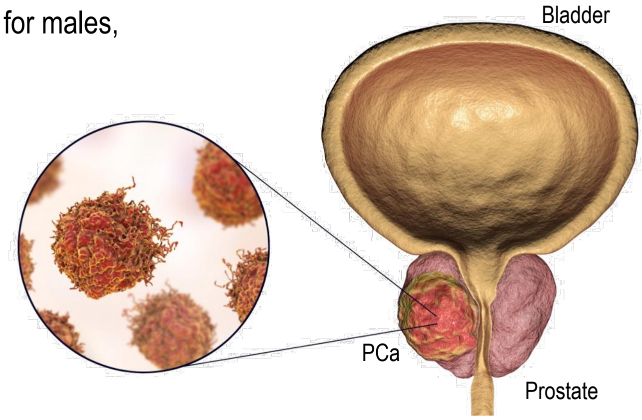

7

† Siegel, R. L., *et al.*, Cancer statistics, 2016. *CA: A Cancer Journal for Clinicians* **66**, 7 30 (2016).

7

Clinical US imaging of PCa

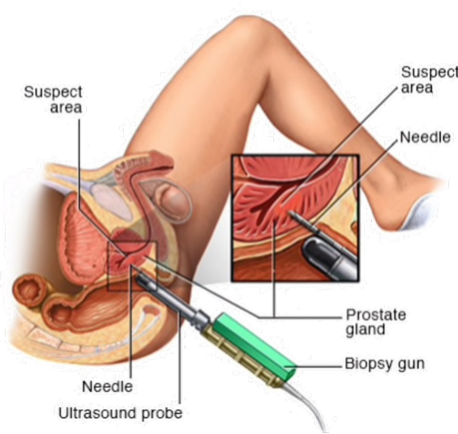

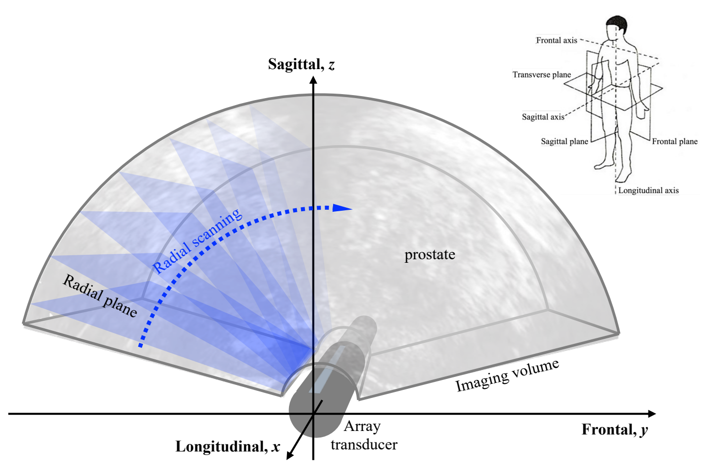

8

8

PCa management in healthcare

Prostate-Specific Antigen (PSA) †

MRI
PET/CT

Transrectal US-guided biopsy

Histopathology

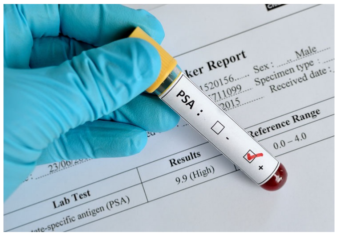

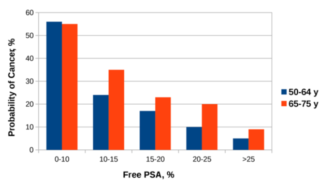

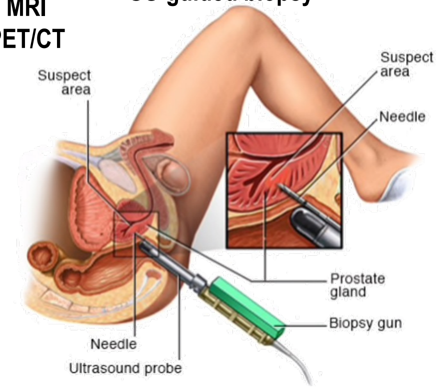

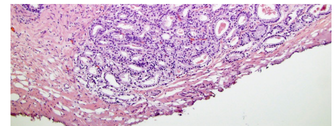

Prostatectomy guidance

- High false-positive rate (75%) †
- The prevalence of nearly invisible PCa on TRUS ranges from 25 to 42% ♀
- Post-operative complications: erectile dysfunction (59.9% at 18M); incontinence (8.4% at 18M)

† Catalona W, *et al.*, *JAMA*. **279** (19): 1542 – 7 (1998).
† Slatkoff S., et al., *J. Fam. Pract.* **60** (6): 357 – 60 (2011).
♀ Piao D., *et al.*, *IEEE J. Selec. Topics in Quantum. Electron.*, **16** (4): 715 – 29 (2009).

9

Mission

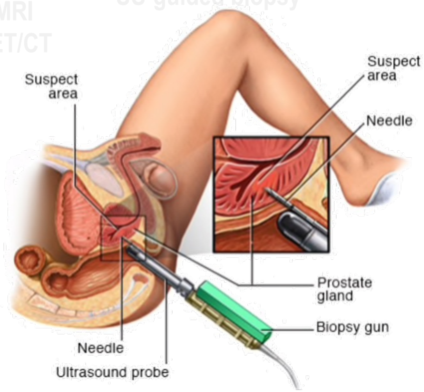

- **Higher spatial resolution**
- **Molecular contrast**

10

Limited aperture, but desire to see more – What shall we do?

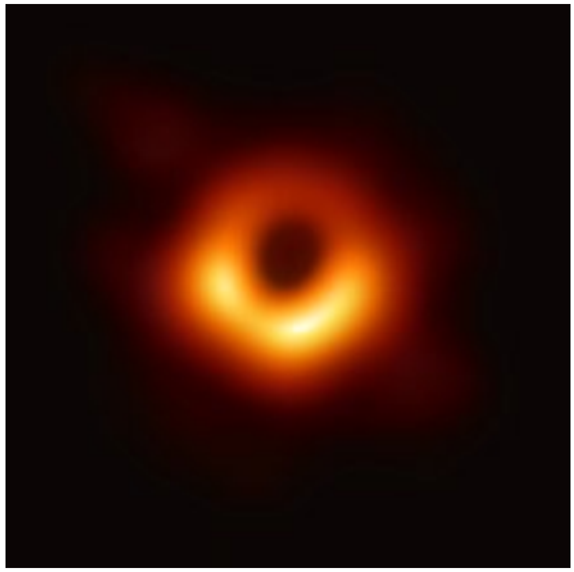

11

11

Synthetic aperture focusing?

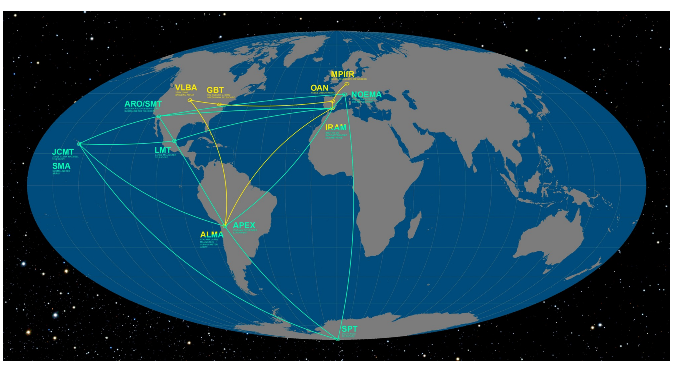

Event Horizon Telescope

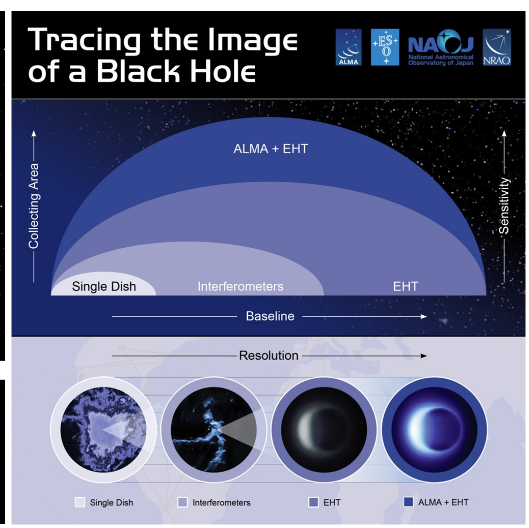

12

12

Synthetic "lateral" aperture focusing in medical ultrasound

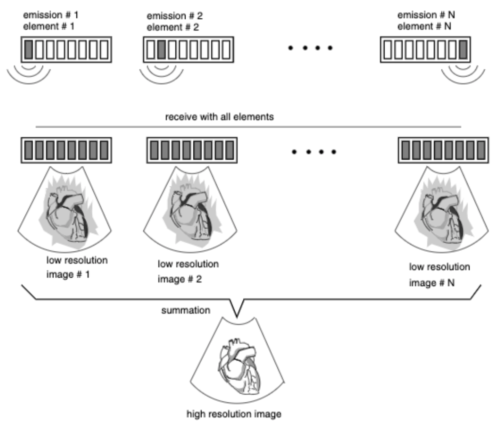

Fig. 1. Basic principle of synthetic aperture ultrasound imaging (from [25]).

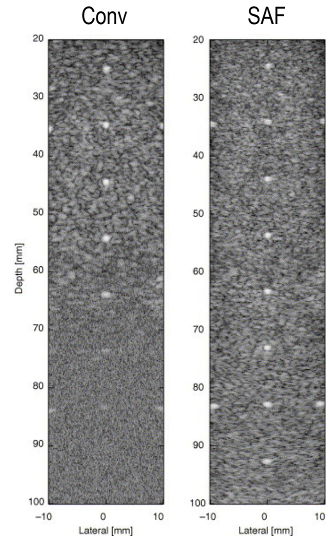

† Bae, S., Kim, P., Song, T. K., *J Acou Soc Am* **144**(5), 2627-2644 (2018).
Chang, J. H., Song, T. K., *IEEE Trans Ultrason Ferroelect, Freq Control* **58**(2), 327-337 (2011).

13

13

Forget about something?

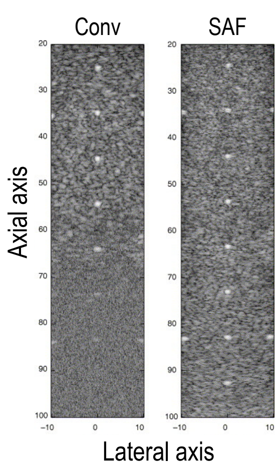

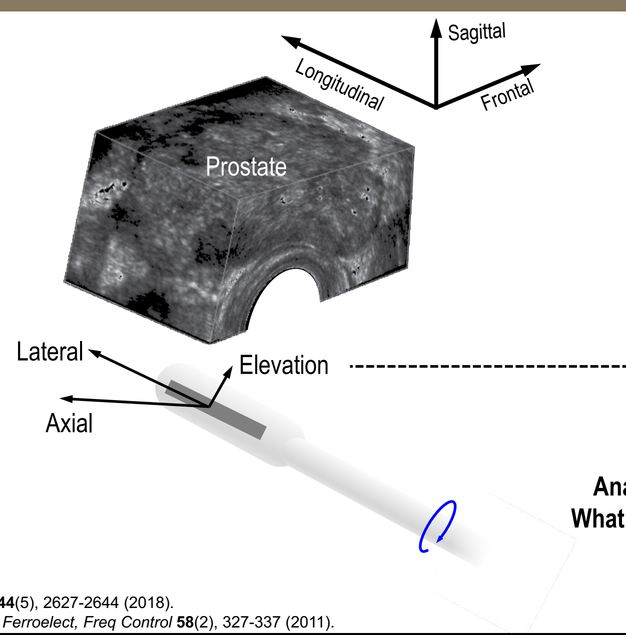

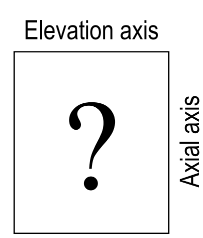

Analytically describable?
What are critical parameters?
How to optimize?

† Bae, S., Kim, P., Song, T. K., *J Acou Soc Am* **144**(5), 2627-2644 (2018).
Chang, J. H., Song, T. K., *IEEE Trans Ultrason Ferroelect, Freq Control* **58**(2), 327-337 (2011).

14

14

Synthetic "radial" aperture focusing (rSAF)

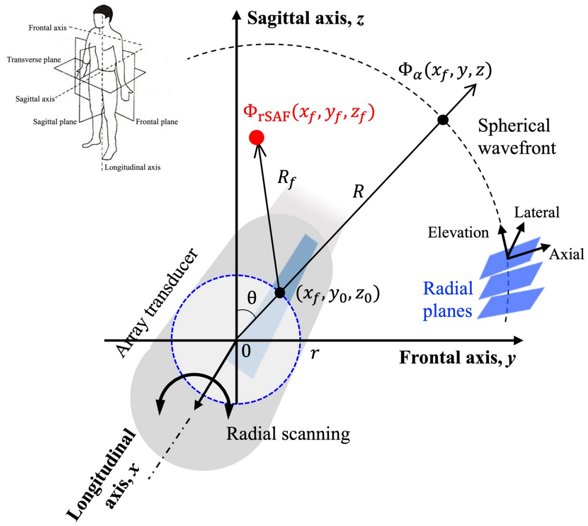

Acoustic field expression of single transmission

$$\Phi_\alpha(y,z,t) = \frac{e^{-j\omega t}}{j\lambda\|R\|_2}\Psi_\alpha(y,z)$$

Continuous transmit beam pattern at a depth of R

$$\Psi_\alpha(y,z) = e^{jkR} = e^{jk\sqrt{(y-r\alpha)^2+(z-r\beta)^2}}$$

Transducer parameters: $r = \sqrt{y_o^2 + z_0^2}$, $k = 2\pi/\lambda$

Scanning parameters: $\theta = \sin^{-1}\alpha$, $\beta = \cos\theta$

Synthetic transmit aperture focused beam pattern at (y_f, z_f)

$$\Psi_{\mathrm{rSAF}}(y_f,z_f) = c_0\int_{-\infty}^{\infty} p_s(\alpha)\tau(\alpha)\Psi_\alpha(y,z)d\alpha$$

Scale factor: $c_0 = \frac{1}{j\lambda\|R\|_2}$

Synthetic focusing delay: $\tau(\alpha) = e^{-jk\sqrt{(y_f-r\alpha)^2+(z_f-r\beta)^2}}$

† H. Song, **J. Kang***, *J Comput Des Eng* **9**, 1774-1787 (2022).
J. Kang, et al., US Patent 63/355,525 (2022).

15

15

Analytical solution for synthetic radial aperture focusing (rSAF)

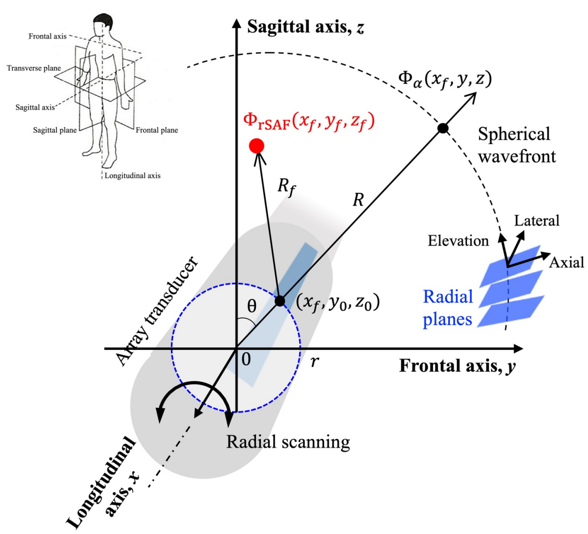

Synthetic transmit aperture focused beam pattern

$$\Psi_{\mathrm{rSAF}}(y_f,z_f) = c_0\int_{-\infty}^{\infty} p_s(\alpha)\tau(\alpha)\Psi_\alpha(y,z)d\alpha,$$

$$\tau(\alpha) = e^{-jk\sqrt{(y_f-r\alpha)^2+(z_f-r\beta)^2}}$$

$$\Psi_\alpha(y,z) = e^{jkR} = e^{jk\sqrt{(y-r\alpha)^2+(z-r\beta)^2}}$$

$$\Psi_{\mathrm{rSAF}}(y_f,z_f) = c_0\int_{-\infty}^{\infty} p_s(\alpha)e^{jk(R-R_f)}d\alpha.$$

Fresnel approximation

$$R - R_f = \frac{y^2 - y_f^2}{2z_f} + \frac{r(y-y_f)}{z_f}\alpha$$

$$\Psi_{\mathrm{rSAF}}(y_f,z_f) = c_0 e^{jk\frac{y^2-y_f^2}{2z_f}}\mathcal{F}[p_s(\alpha)]\Big|_{f_y=\frac{ry'}{\lambda z_f}} \qquad y' = y - y_f$$

† H. Song, **J. Kang***, *J Comput Des Eng* **9**, 1774-1787 (2022).
J. Kang, et al., US Patent 63/355,525 (2022).

16

16

Analytical solution for synthetic radial aperture focusing (rSAF)

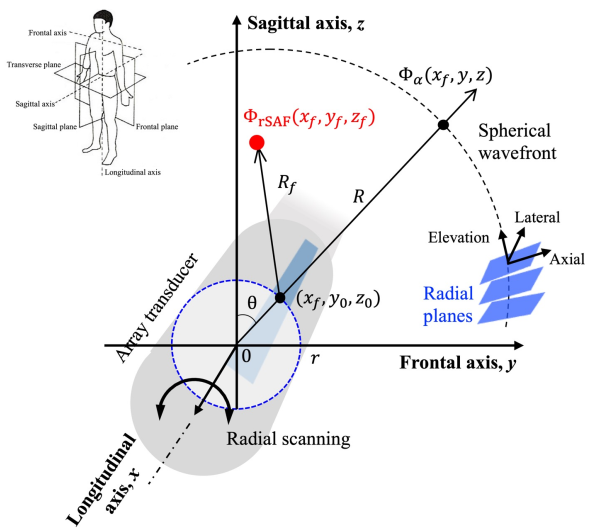

Discrete synthetic transmit aperture focused beam pattern

$$\Psi_{\mathrm{rSAF}}(y_f,z_f)=c_0 e^{jk\frac{y^2-y_f^2}{2z_f}}\mathcal{F}[p_s(\alpha)]\Big|_{f_y=\frac{ry'}{\lambda z_f}}$$

$$p'_s(\alpha)=\sum_{n=0}^{N-1}\delta(\alpha-\alpha_n)$$

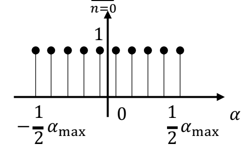

$$\Psi_{\mathrm{rSAF}}(y_f,z_f)=c_1'\frac{\sin\pi\frac{rN\Delta\alpha}{\lambda z_f}y}{\sin\pi\frac{r\Delta\alpha}{\lambda z_f}y}$$

Revised scale factor

$$c_1'=c_0\cdot e^{jk\frac{y^2-y_f^2+r\alpha_{\max}}{2z_f}y}$$

Null-to-null beam width

$$y'_{s\,\mathrm{ML}}=\frac{\lambda z_f}{rN\Delta\alpha}=\frac{\lambda z_f}{r\alpha_{\max}}$$

Grating lobe positions

$$y'_{s\,\mathrm{GL}}=\frac{\lambda z_f}{r\Delta\alpha}n$$
$(n=1,2,\ldots)$

† H. Song, **J. Kang***, *J Comput Des Eng* **9**, 1774-1787 (2022).
J. Kang, et al., US Patent 63/355,525 (2022).

17

17

Practical implementation strategy

Virtual source-based SAF technique‡

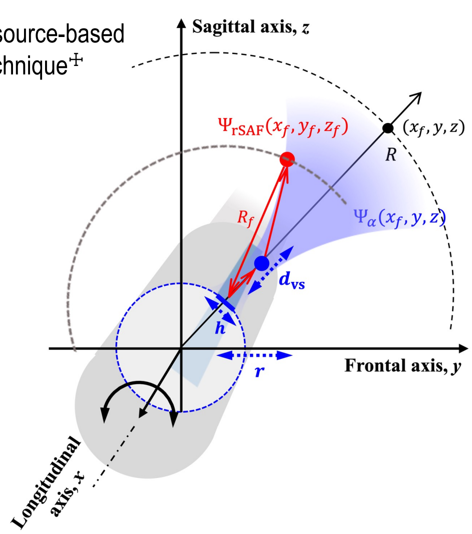

Synthetic aperture focusing delay calculation

Transmit
$d_t(i,z)=d_{VS}+d_{tf}(i,z)$
$\tau_t(i,z)=d_t(i,z)/c$

Receive
$\tau_r(z)=d_r(z)/c$
(i.e., R_f)

$$\tau_f(i,z)=\tau_t(i,z)+\tau_r(z)$$

Radial aperture synthesis

$$I_{\mathrm{rSAF}}(\theta_n,z)=\frac{1}{N_{\mathrm{syn}}(z)}\sum_{i=n-N_{syn}(\theta_n,z)/2+1}^{n+N_{syn}(\theta_n,z)/2} I_i(\theta_n,\tau_f(i,z))$$

† H. Song, **J. Kang***, *J Comput Des Eng* **9**, 1774-1787 (2022).
J. Kang, et al., US Patent 63/355,525 (2022).
‡ Frazier C. H., et al., *IEEE Trans Ultrason Ferroelect Freq Control*, **45**(1), (1998)

18

18

Design framework

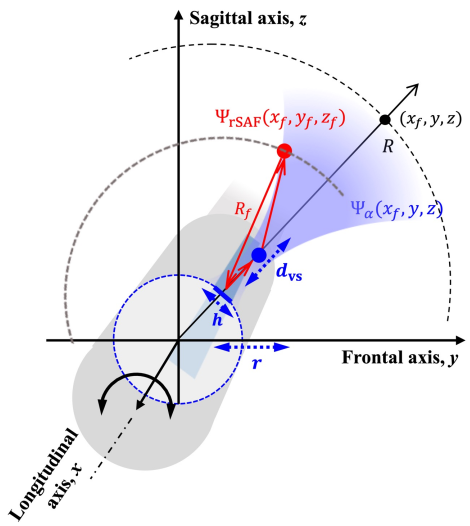

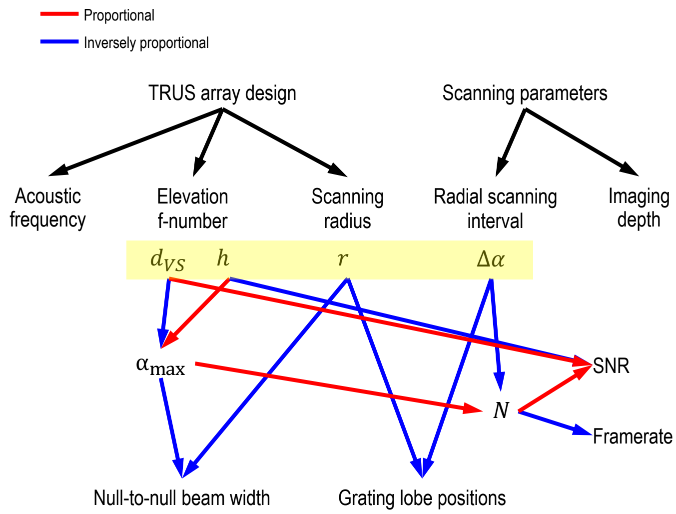

$y'_{s\,\mathrm{ML}} = \dfrac{\lambda z_f}{r\alpha_{\max}}$

$y'_{s\,\mathrm{GL}} = \dfrac{\lambda z_f}{r\Delta\alpha} n \; (n = 1,2,3, \ldots)$

† H. Song, **J. Kang***, *J Comput Des Eng* **9**, 1774-1787 (2022).
J. Kang, et al., US Patent 63/355,525 (2022).

19

19

Spatial resolution & grating lobe

d_{VS} = 5 mm; h = 7 mm

$y'_{s\,\mathrm{GL}} = \dfrac{\lambda z_f}{r\Delta\alpha} n \; (n = 1,2,3, \ldots)$

$y'_{s\,\mathrm{ML}} = \dfrac{\lambda z_f}{r\alpha_{\max}}$

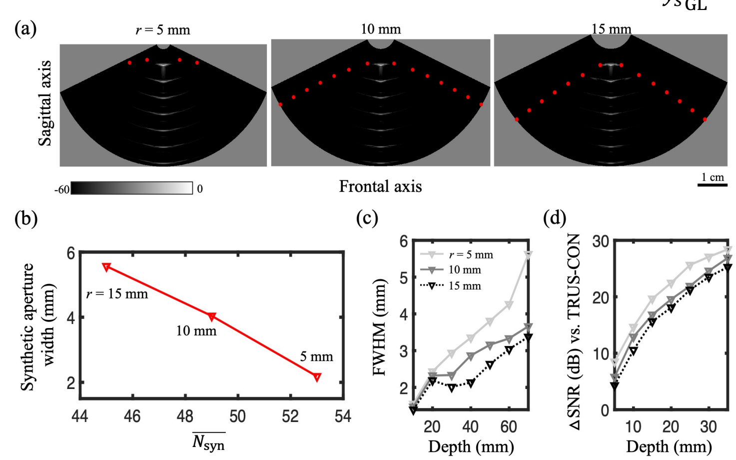

† H. Song, **J. Kang***, *J Comput Des Eng* **9**, 1774-1787 (2022).
J. Kang, et al., US Patent 63/355,525 (2022).

20

20

2D Field-II simulation – Frontal-sagittal plane

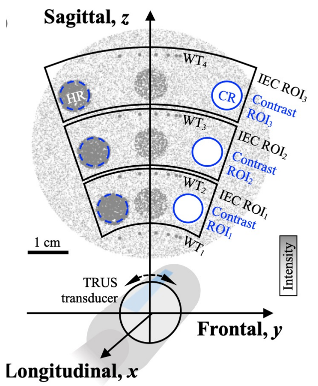

† H. Song, **J. Kang***, *J Comput Des Eng* **9**, 1774-1787 (2022).
J. Kang, et al., US Patent 63/355,525 (2022).

Comparison to clinical standard

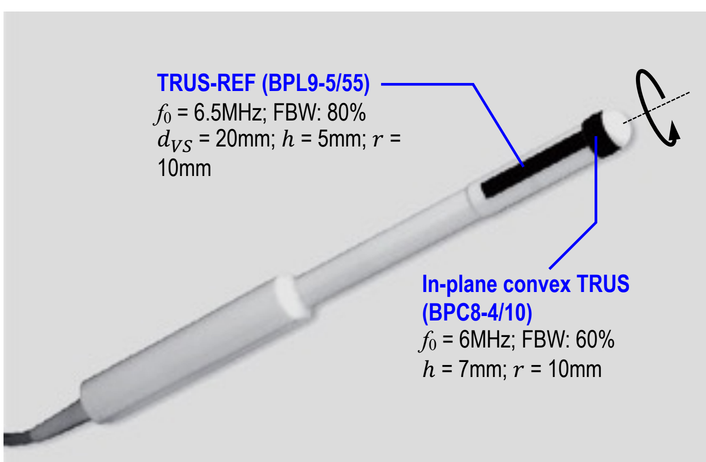

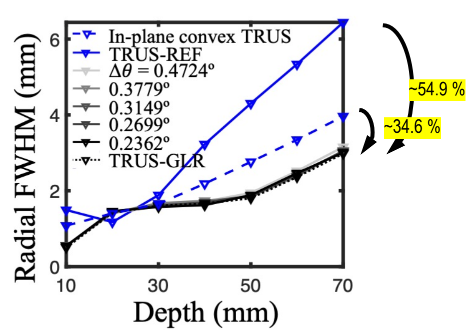

† H. Song, **J. Kang***, *J Comput Des Eng* **9**, 1774-1787 (2022).
J. Kang, et al., US Patent 63/355,525 (2022).

What's next?

Null-to-null beam width

$$y'_{s\,\mathrm{ML}} = \frac{\lambda z_f}{r\alpha_{\max}}$$

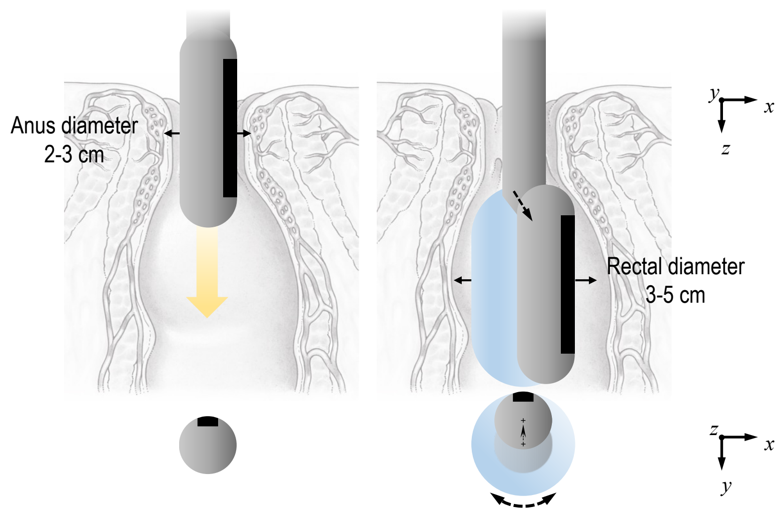

† H. Song, **J. Kang***, *J Comput Des Eng* **9**, 1774-1787 (2022).
J. Kang, et al., US Patent 63/355,525 (2022).

23

23

What's next?

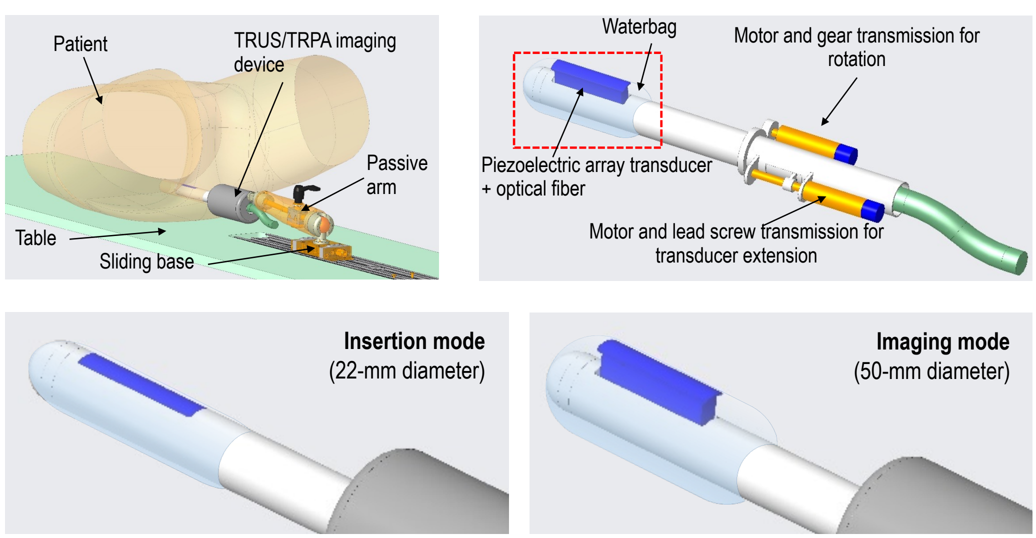

Courtesy of Dr. Iulian Iordachita
† H. Song, **J. Kang***, *J Comput Des Eng* **9**, 1774-1787 (2022).
J. Kang, et al., US Patent 63/355,525 (2022).

24

24

Summary

- TRUS-rSAF technique can provide **unprecedented volumetric spatial resolution** higher than clinical convex/linear TRUS array transducer
- Analytical description and optimization framework were developed
- Mechatronic implementation will provide a next-generation TRUS imaging for higher sensitivity and specificity to detect and diagnose PCa
- Further works: prototyping & clinical translation

25

25

Mission

Prostate-Specific Antigen (PSA) [†] → MRI PET/CT → Transrectal US-guided biopsy → Histopathology → Prostatectomy guidance

- High false-positive rate (75%) [†]

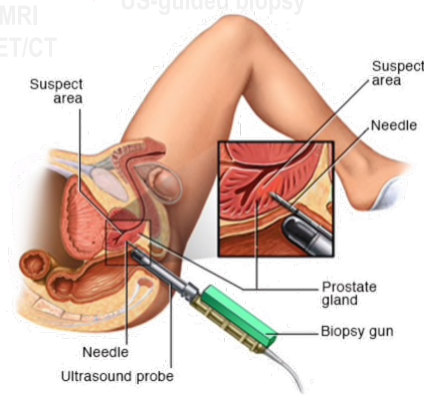

- The prevalence of nearly invisible PCa on TRUS ranges from 25 to 42% [♀]

- **Higher spatial resolution**
- **Molecular contrast**

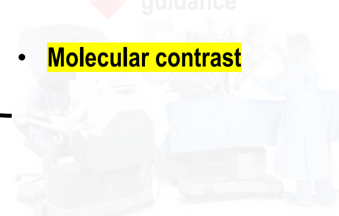

- Post-operative complications: erectile dysfunction (59.9% at 18M); incontinence (8.4% at 18M)

† Catalona W, *et al.*, *JAMA*. **279** (19): 1542 – 7 (1998).
† Slatkoff S., et al., *J. Fam. Pract.* **60** (6): 357 – 60 (2011).
♀ Piao D., *et al.*, *IEEE J. Selec. Topics in Quantum. Electron.*, **16** (4): 715 – 29 (2009).

26

Prostate-Specific Membrane Antigen (PSMA)

- Type-II integral cell-surface membrane protein †
- Overexpressed in nearly all solid tumors (e.g., breast, bladder, pancreatic, testicular, or colorectal cancers) †
- **High correlation to PCa aggressiveness**, implying its functional role in PCa biology ♀

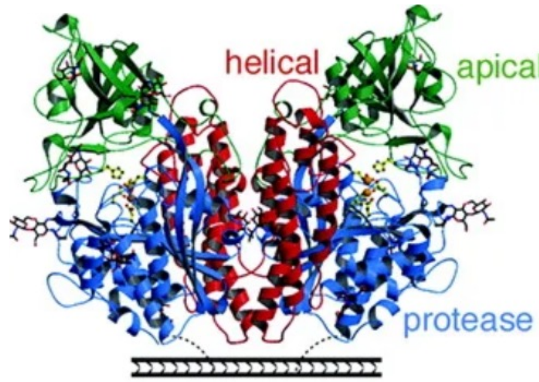

Ribbon diagrams of side view of PSMA †

† Davis M.I., et al., *PNAS* **102** (17): 5981 – 86 (2005); Balk S.P., *et al.*, *J. Clin. Oncol.* **21** (2): 383–91 (2013).
† Neuman B. P., et al., *Clin. Cancer Res.* **21** (4): 771 – 80 (2014).
♀ Minner S., et al., *Prostate* **71** (3), 281 – 8 (2011).

27

27

Targeting PSMA for early-PCa detection

PET/MRI/CT †
Pros: Wide field-of-view across whole-body; High specificity
Cons: Iodizing effects; Slow imaging speed; expensive

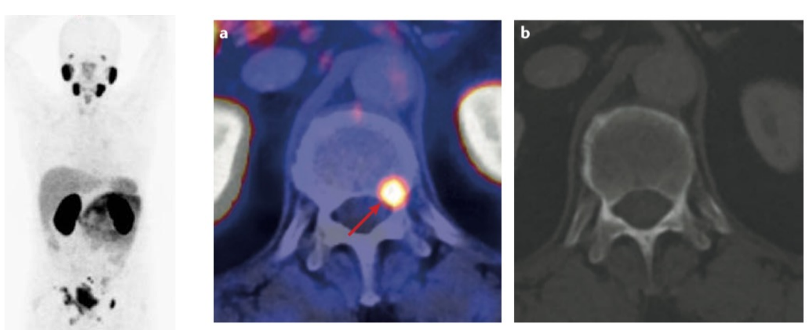

Extensive clinical trials stages I and II: NCT02282137, NCT02611882, NCT02488070, NCT02048150, NCT01173146 …

Optical imaging † …
Pros: Real-time; easy to use
Cons: Superficial sensing depth

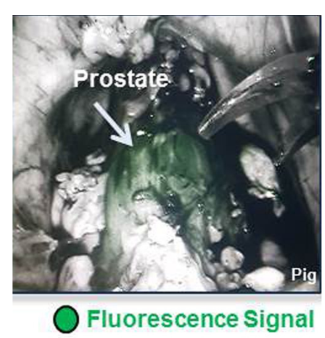

Clinical trials in IND stage: NCT01173146, NCT02048150

† Maurer T., et al., *Nat. Rev. Urol.* **13**: 226 – 35 (2016).
† Zhang R.R., et al., *Nat. Rev. Clin. Oncol.* **14** (6): 347 – 64 (2017); Baranski A.-C., *et al.*, *J. Necl. Med.*, **59** (4): 639 – 45 (2018).

28

28

Adding light: biomedical photoacoustics

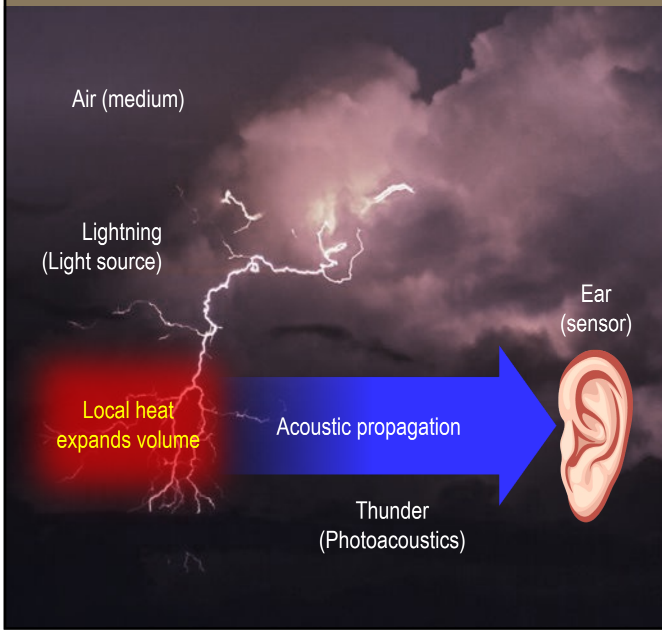

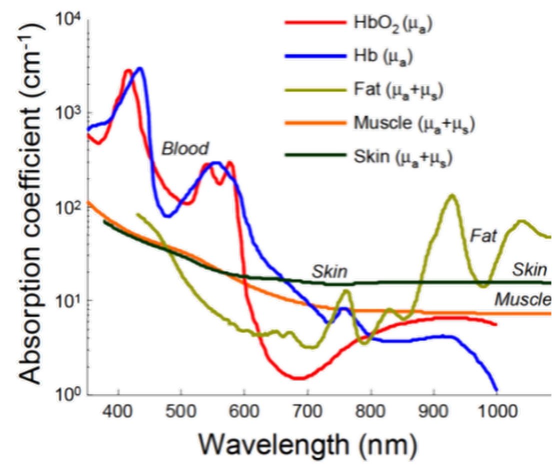

† L. V. Wang, S. Hu, *Science* **6075** (2012).
J. Kang, *et al.*, *Exp Neurol* **347** (2022).

29

29

Competitive analysis

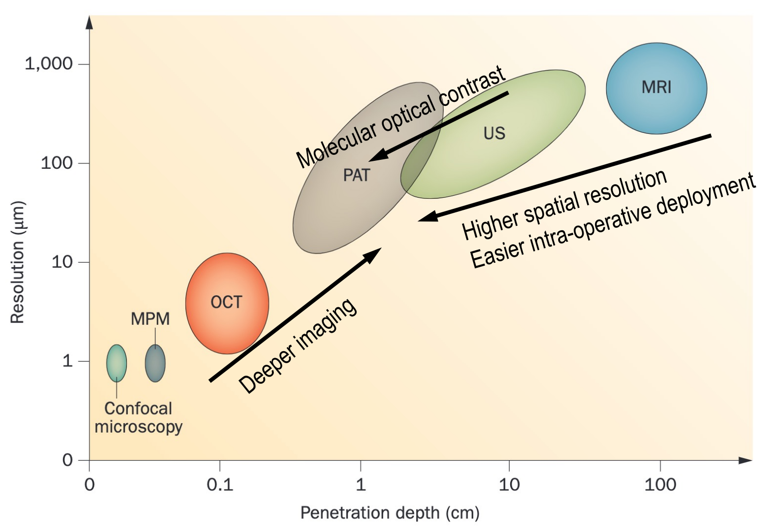

† Reproduced from
Fried N. M., Burnett A. L., Nat Urol Rev 12, 451-460 (2015).

30

30

Multi-functional PSMA-targeted platform

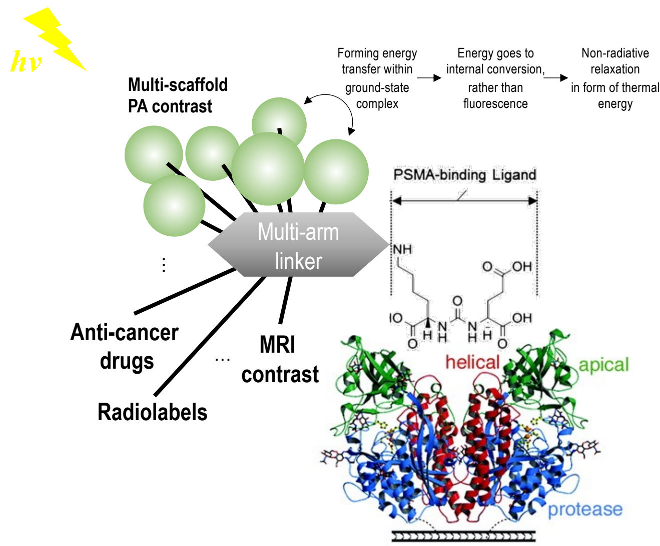

† [Zhang H.K., Chen Y.], **J. Kang**, *et al.*, *J. Biophotonics* **11**:e201800021 (2018).
[Lesniak, W., Wu, Y.], **J. Kang**, et al., *Nanoscale* **13**(20), 9217-9228 (2021).

31

31

Second-generation PSMA-targeting agent

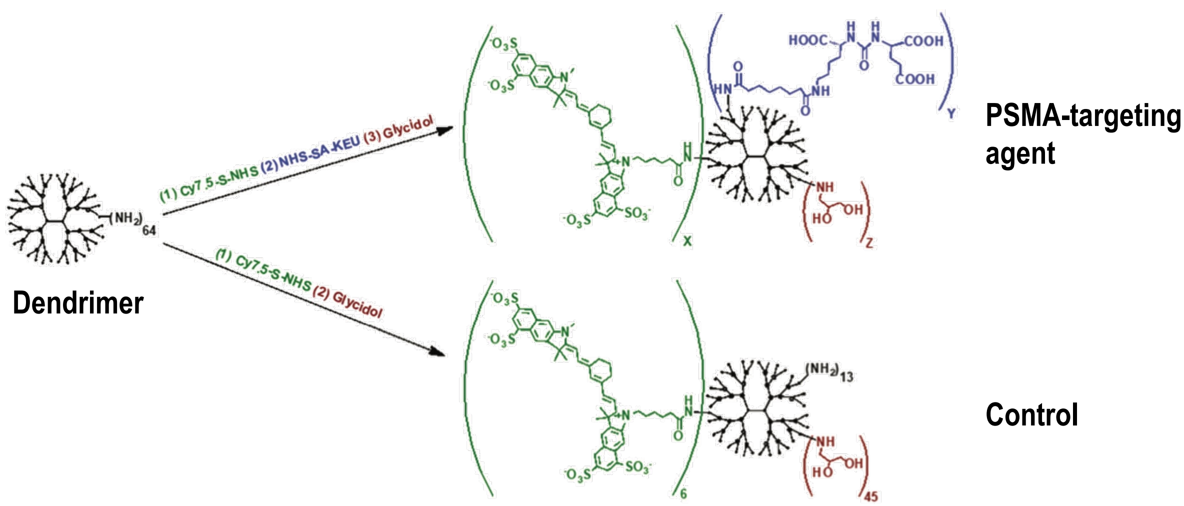

† [Zhang H.K., Chen Y.], **J. Kang**, *et al.*, *J. Biophotonics* **11**:e201800021 (2018).
[Lesniak, W., Wu, Y.], **J. Kang**, et al., *Nanoscale* **13**(20), 9217-9228 (2021).

32

32

In vivo PA-based PSMA-targeted imaging

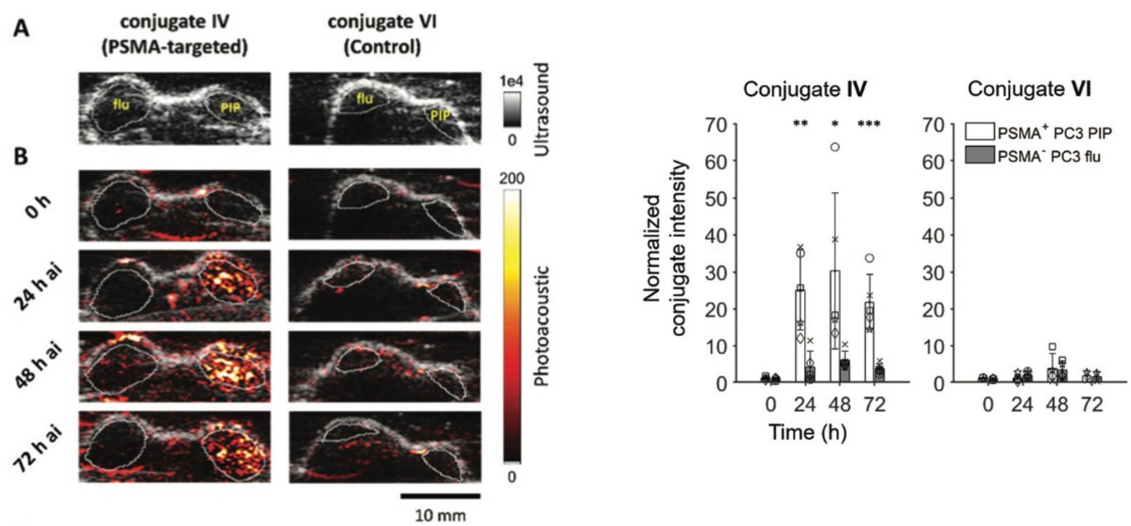

† [Lesniak, W., Wu, Y.], **J. Kang**, et al., *Nanoscale* **13**(20), 9217-9228 (2021).

33

33

Potential engineering pitfalls

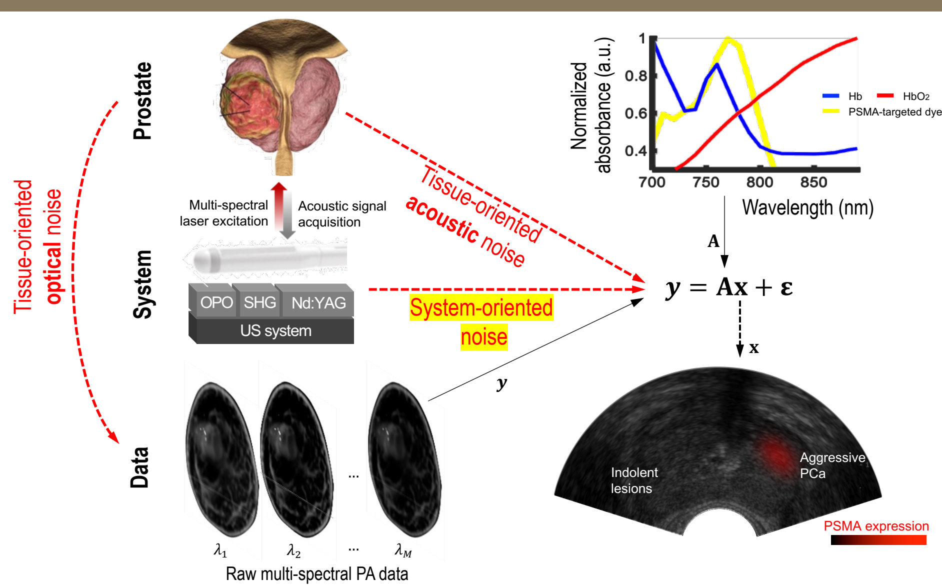

† **[Wu, Y., Kang, J.]**, *Photoacoustics* **27**, 100378 (2022).

34

34

Spectral system noise segregation

$\mathbf{y}$

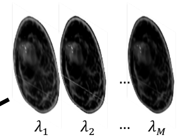

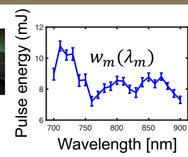

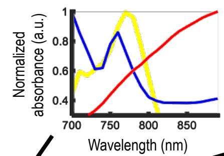

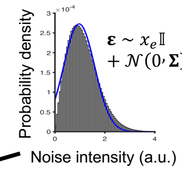

$$y = \mathbf{A}\mathbf{x} + \boldsymbol{\varepsilon}$$

$$\mathbf{y} = \mathbf{W}^{-1}\mathbf{y} = \mathbf{W}^{-1}(\boldsymbol{s} + \boldsymbol{\varepsilon})$$

$$\mathbf{y} = [\mathbf{A} \mid \mathbf{v}] \begin{bmatrix} \mathbf{x} \\ x_e \end{bmatrix} + \boldsymbol{\varepsilon} = \mathbf{Q}\mathbf{x} + \boldsymbol{\varepsilon}$$

$\mathrm{diag}(\mathbf{v}) = \mathbf{W}^{-1}$ $\quad$ $\mathbf{x} \in \mathbb{R}^{N+1}$, $\boldsymbol{\varepsilon} \sim \mathcal{N}(0, \boldsymbol{\Sigma})$

Non-negative least squares (NNLS) using quadratic programming techniques

$$\underset{\mathbf{x} \geq 0}{\arg\min} \left(\frac{1}{2} \mathbf{x}^{\mathrm{T}} \mathbf{A}^{\mathrm{T}} \mathbf{A} \mathbf{x} - \mathbf{y}^{\mathrm{T}} \mathbf{A} \mathbf{x} \right)$$

$$\underset{\mathbf{x} \geq 0}{\arg\min} \left(\frac{1}{2} \mathbf{x}^{\mathrm{T}} \mathbf{Q}^{\mathrm{T}} \mathbf{Q} \mathbf{x} - \boldsymbol{y}^{\mathrm{T}} \mathbf{Q} \mathbf{x} \right)$$

35

† **[Wu, Y., Kang, J.]**, *Photoacoustics* **27**, 100378 (2022).

35

In vivo validation

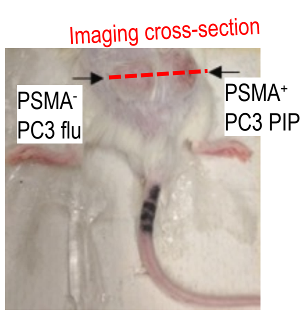

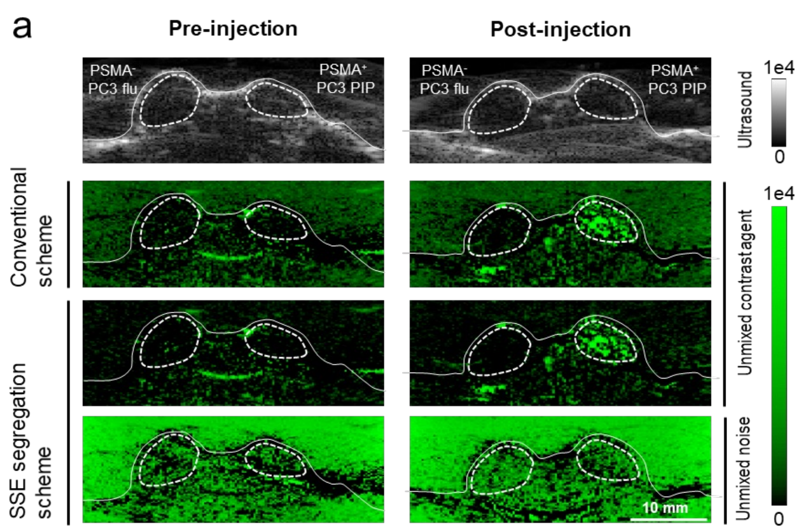

36

† **[Wu, Y., Kang, J.]**, *Photoacoustics* **27**, 100378 (2022).

36

In vivo validation

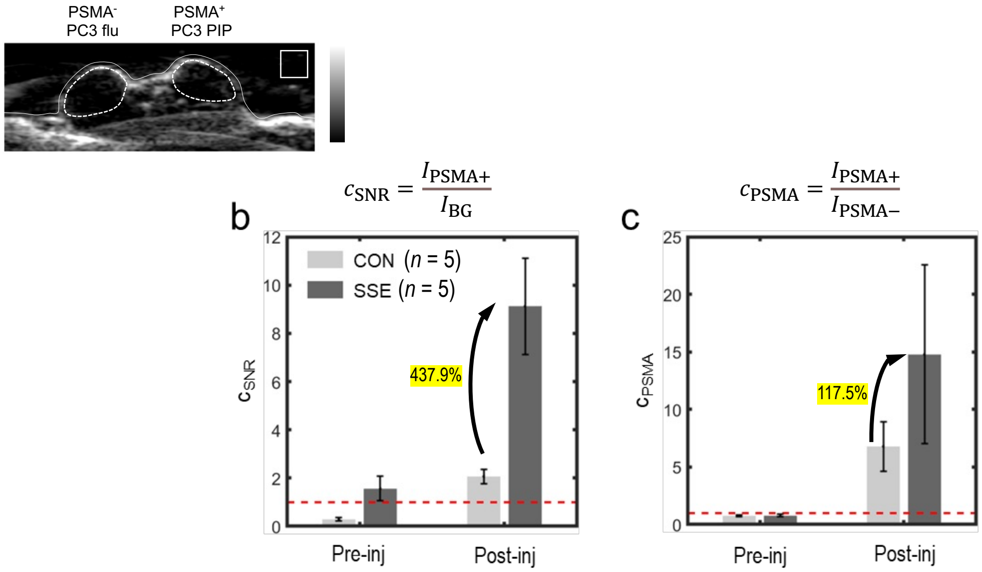

† [Wu, Y., Kang, J.], *Photoacoustics* **27**, 100378 (2022).

37

37

Summary

- PSMA-targeted imaging may endow new possibility to provide **molecular contrast exclusively on aggressive PCa using TRUS/PA imaging**
- **Dedicated signal processing algorithms** (spectral system noise, wavelength optimization, frame averaging) will enhance the clinical sensitivity and specificity
- Furter works
  - Multi-functional (theranostics), multi-modal (PA/US + MRI or PET) imaging capability will be developed.
  - Multi-institutional team for animal model and clinical testing is in preparation (NIH, Hopkins).

38

38

Remarks

Transformable TRUS/PA imaging

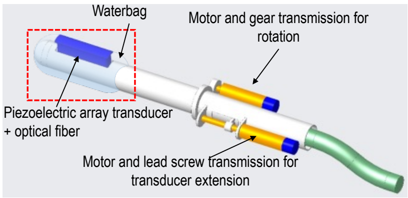

TRUS/PA diagnostics & interventional guidance

- Expanded role in PCa diagnostics
- Microtumor detection (3-5 mm → 1-2 mm)
- High-accuracy biopsy guidance, targeting PSMA expression

PSMA-targeted imaging

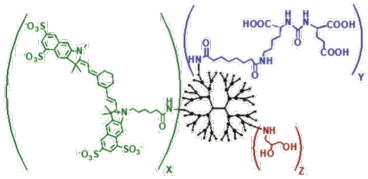

Signal processing algorithm

$$\underset{\mathbf{x}\geq 0}{\arg\min}\left(\frac{1}{2}\mathbf{x}^{\mathrm{T}}\mathbf{Q}^{\mathrm{T}}\mathbf{Q}\mathbf{x}-\boldsymbol{y}^{\mathrm{T}}\mathbf{Q}\mathbf{x}\right)$$

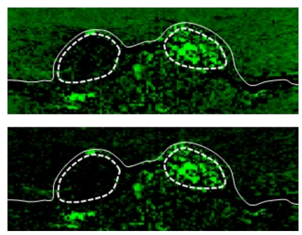

39

Complication of radical prostatectomy

- **Erectile dysfunction** is a post-operative complication of radical prostatectomy
- Current nerve-sparing techniques only consider neurovascular bundle (NVB), excluding cavernous nerve branches
- **Only 60-85% of PCa patients recover erectile function, and early recovery is uncommon (up to 2 years)** †

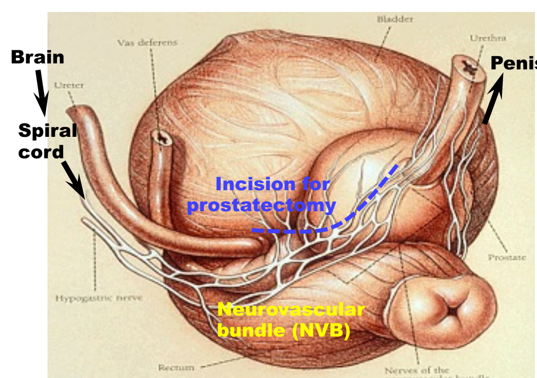

Nerve system surrounding prostatic gland ‡

40

† A. L. Burnett, *JAMA* **293**(21), 2648--2653 (2005).
‡ https://www.virginiamason.org/radical-prostatectomy

Current state-of-the-art

Fluorophore-based fluorescence imaging †

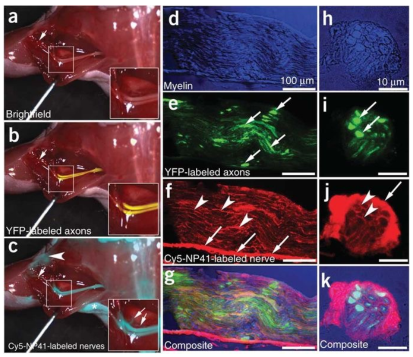

- Concern on tissue toxicity
- Long staining time (2hr – 14 days)

Coherent anti-Strokes Raman spectroscopy

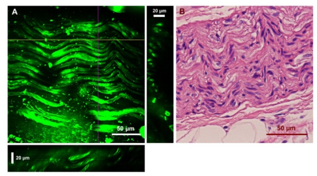

- Slow imaging
- Limited imaging depth

Confocal and Multiphoton microscopy

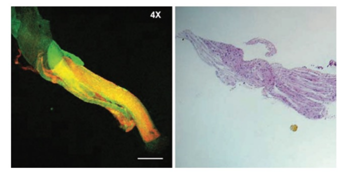

- Not optimized for intra-operative use
- Limited imaging depth

Optical coherence tomography (OCT) ‡

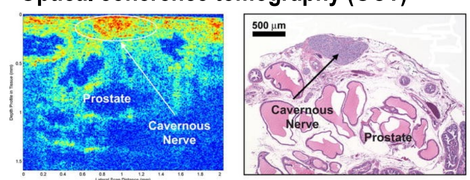

- Lack of nerve-specific contrast
- Limited contrast resolution due to speckle artifacts

Prostate MRI §

- Slow speed
- Not portable

† M. A. et al. *Nat Biotechnol* **29**, 352–356 (2011).
‡ ChiWhitneytchian, S., et al., *J. Biomed. Opt.* **14**, 014031-14-6 (2009).
§ A. L. Burnett, *Nat. Rev. Urol.* **12**, 451-460 (2015).

41

41

Near-infrared VSD mechanism

- Transmembrane redistribution mechanism †,‡

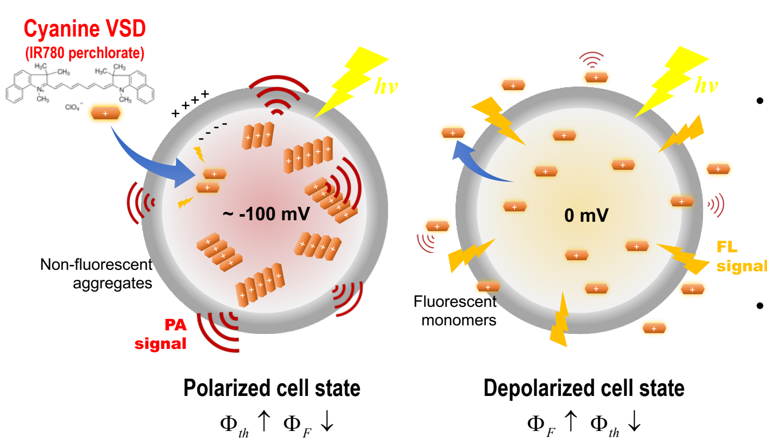

- Polarized cell state
  - Cyanine dye positively charged is attracted into cell membrane
  - The aggregation of VSD leads to fluorescence (FL) quenching, which **increases PA efficiency**
- Depolarized cell state
  - Dispersion of VSD gives **high FL efficiency**

42

† Zhang, H. K., **Kang, J.**, *et al.* *J. Biomed. Opt.* **22,** 045006 (2017).

42

Near-infrared VSD characterization

- Artificial membrane diffusion potential model [†,‡]

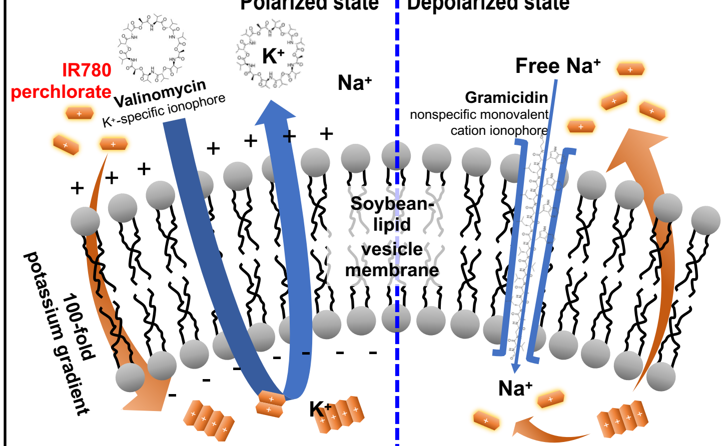

In vitro VSD characterization (6μM). (A) Absorbance and fluorescence emission spectrum of near-infrared VSD. (B) Photoacoustic spectrum and intensity change at the 790 nm of peak absorbance. [§]

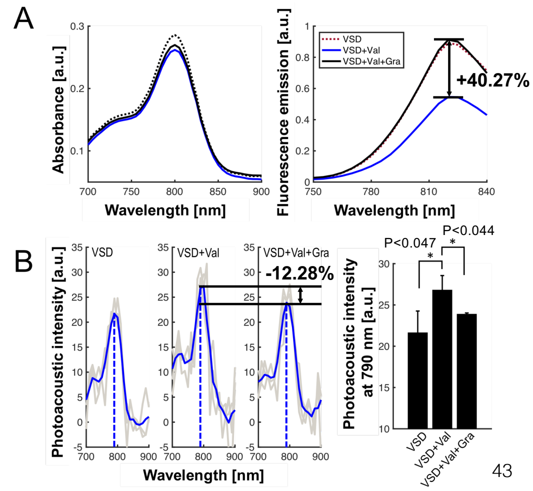

† Gross, E., et al. *Biophys. J.* **67**, 208-216 (1994)
‡ Zhang, H. K., **J. Kang**, *et al. J. Biomed. Opt.* **22,** 045006 (2017).
§ **J. Kang**, et al., *Front Neurosci* **13**(579), 1-14 (2019)

43

43

Preliminary evidence of neural sensing

Non-invasive epileptic seizure detection †

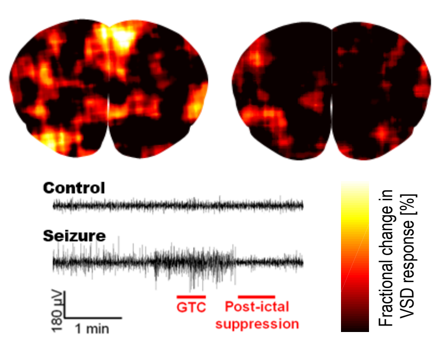

Non-invasive characterization of excitatory neurotransmittance at rat hippocampus ‡

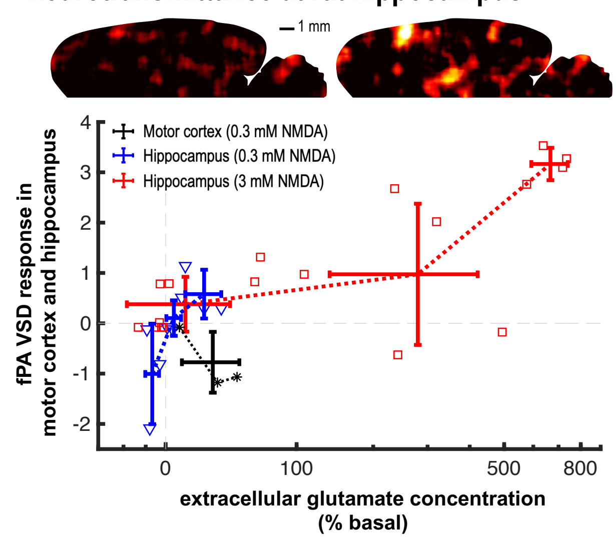

† **J. Kang**, *et al., Front Neurosci* **13**(579), 1-14 (2019)
‡ **J. Kang**, *et al., J Neural Eng* **17**(2), 025001 (2020).

44

44

Proposed image-guided nerve-sparing laparoscopic radical prostatectomy

- **Objective:** Image-guided nerve guidance with:
  (1) **Real-time functional nerve localization** with high specificity,
  (2) **Short VSD staining duration** (~10 min)
  (3) **Wide field-of-view** familiar with surgeons, and
  (4) **Near-infrared imaging** for better transfascial nerve localization

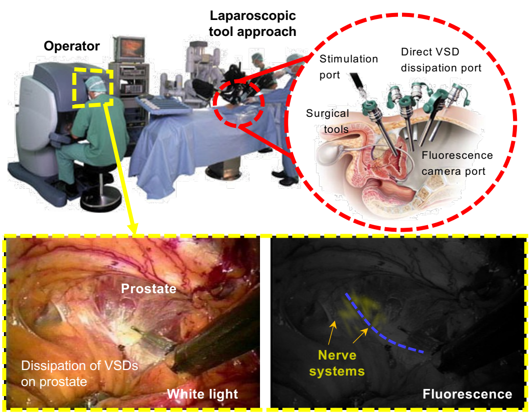

Step 1: Robotic tool approach through the ports on the abdominal incisions,
Step 2: Direct transfascial VSD staining within a time limit up to 10 min,
Step 3: Flushing out of the VSD on the prostate surface which is not bound at tissue membrane,
Step 4: Nerve stimulation for nerve-selective VSD contrast, and
Step 5: Nerve-sparing prostatectomy with the augmented nerve map using intra-operative FL imaging solution

45

† J. Kang, *et al.*, *Sci Rep* **10**, 6618 (2020).

45

In vivo experimental setup: Imaging system and animal preparation

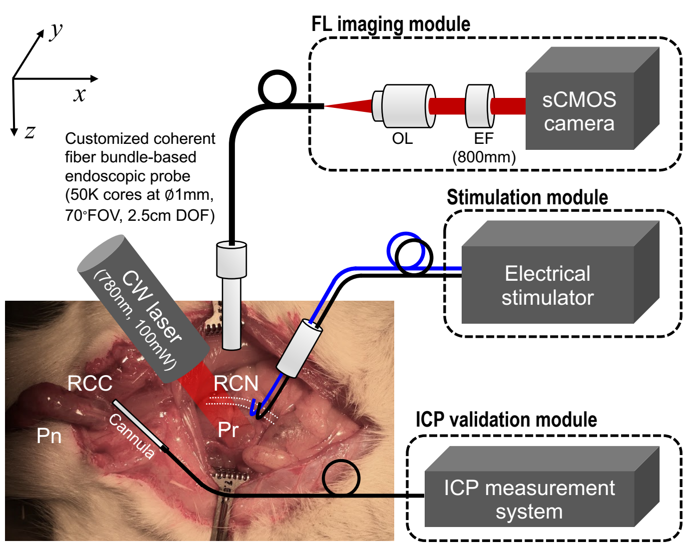

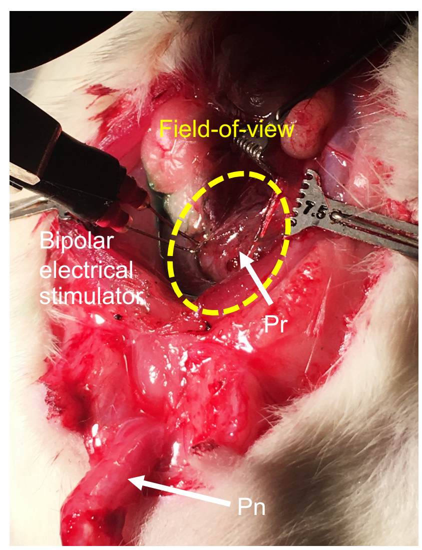

Pr: prostate; Pn: penis; CN: cavernous nerve; RCC: right corpus caverosum; ICP: Intracavernosal pressure

46

† J. Kang, *et al.*, *Sci Rep* **10**, 6618 (2020).

46

In vivo experimental setup: Imaging and stimulation protocol

- Experimental protocol

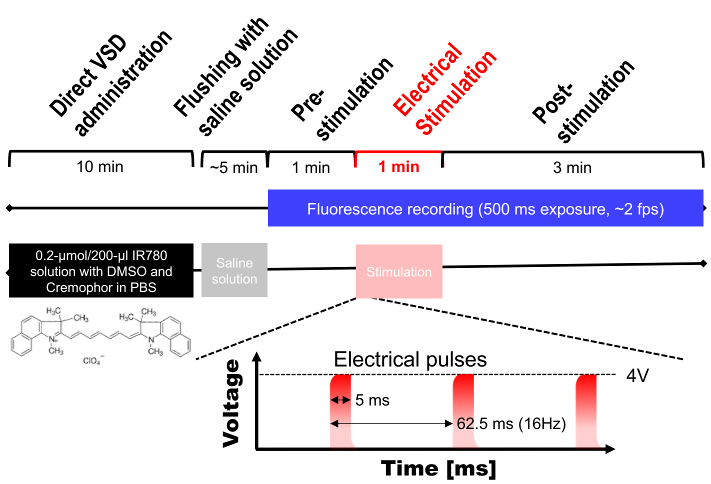

Validation of erectile stimulation

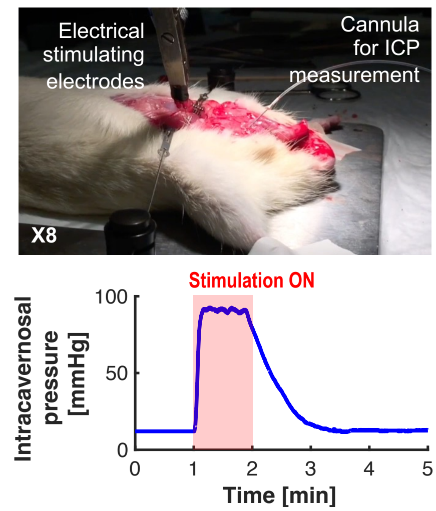

47

† J. Kang, *et al.*, *Sci Rep* **10**, 6618 (2020).

47

Real-time trans-fascial functional prostate nerve mapping *in vivo*

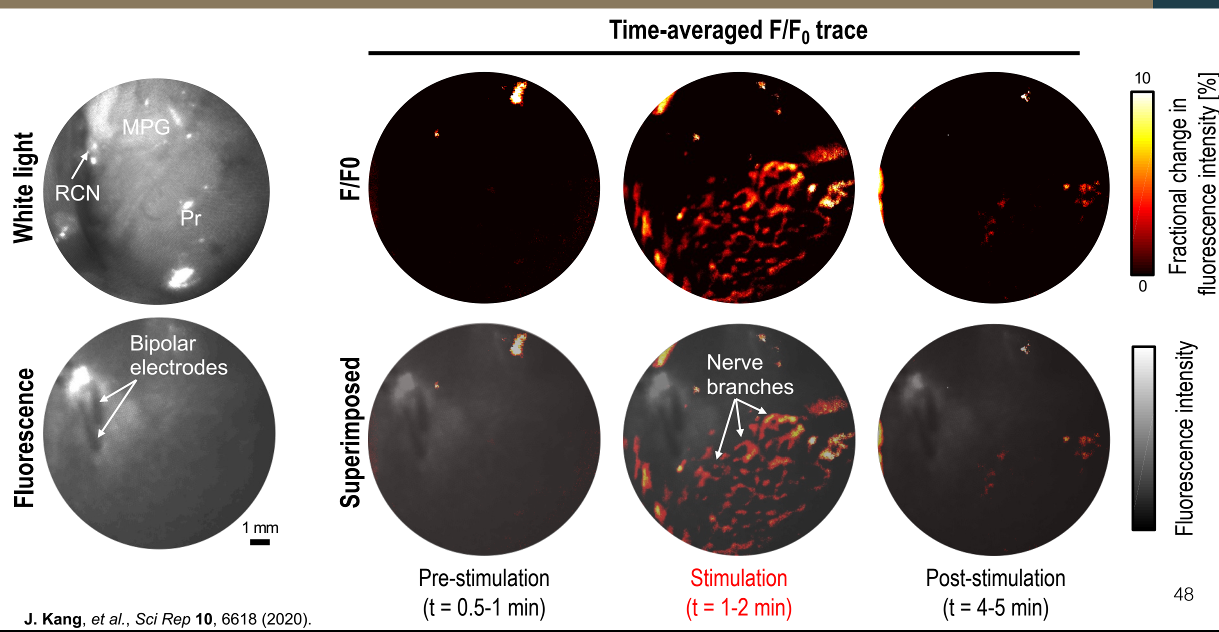

48

† J. Kang, *et al.*, *Sci Rep* **10**, 6618 (2020).

48

Histological validation of direct VSD delivery

- Successful direct VSD staining on nerve layer below prostatic fascia

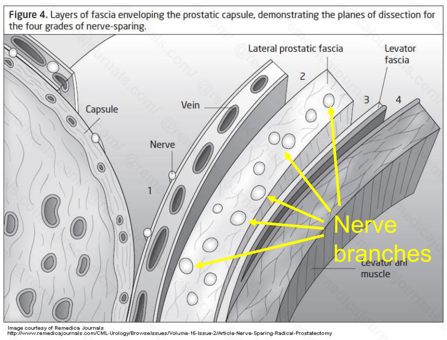

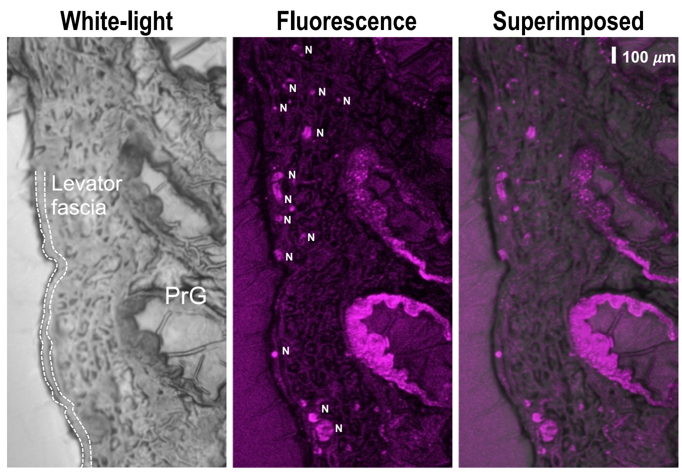

† J. Kang, *et al.*, *Sci Rep* **10**, 6618 (2020).

49

49

Discussion

- We presented the preliminary results of real-time nerve guidance using dual-modal VSD and near-infrared FL imaging
- Our further works will be focused on
  - Collecting more data for statistical rigor
  - Toxicity study and efficiency evaluation with various VSD concentrations
  - Advance experimental setup to induce selective cavernous nerve blocking
  - Developing pulsed laser-based dual-modal intra-operative guidance system
  - *In vivo* large-scale animal study for evaluating clinical outcome (post-operative erectile dysfunction with functional guidance vs. no imaging guidance)

50

50

Defining the right form of “the sixth sense”

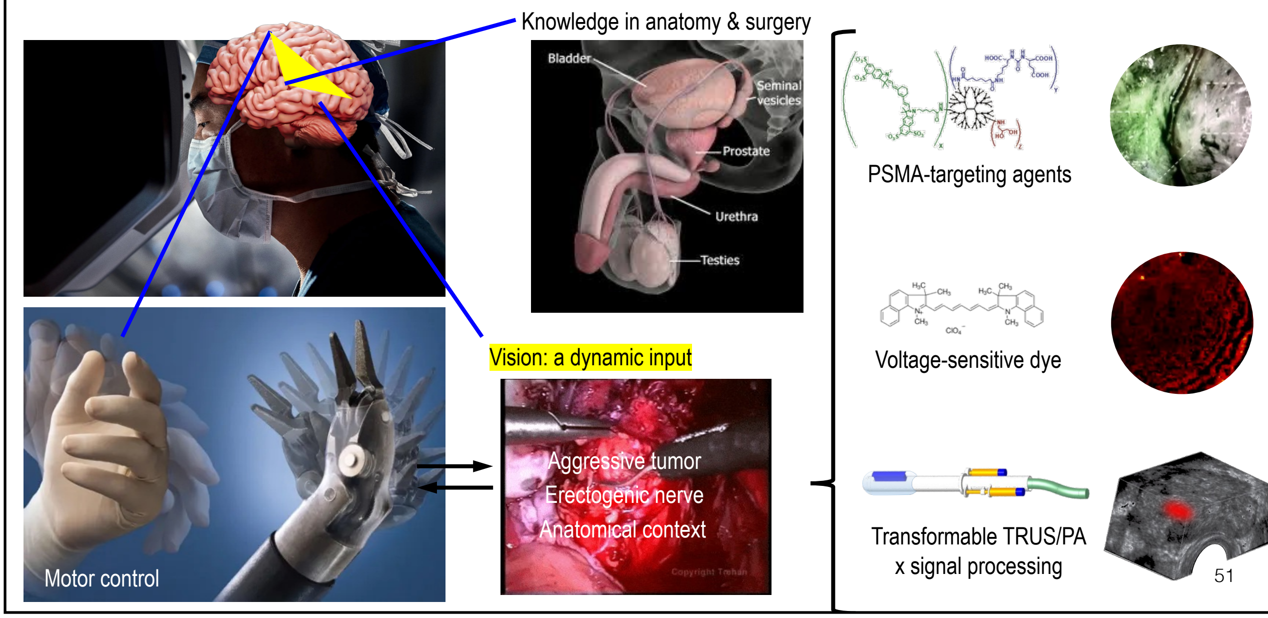

51

Acknowledgement

- CDMRP PCRP W81XWH-18-1-0188 **(PI)**
- NIH Blueprint MedTech Pilot program **(PI)**
- NIH R41 EB033758 **(MPI)**
- NIH R01 HL139543; R24 MH106083
- Discovery award, Johns Hopkins University

NIH National Institutes of Health
Turning Discovery Into Health

CDMRP

Thank you

Johns Hopkins University
Laboratory for Computational Sensing + Robotics
MUSiiC Research Laboratory

52

52